Electronic Supplementary Material (ESI) for Physical Chemistry Chemical Physics.

Ion Molecule Reactions in the HBr^+ + HCl (DCl) System:

A combined experimental and theoretical study

Dominik Plamper, [a] Sebastian Schmidt, [a] Karl-Michael Weitzel,*[a] Kazuumi Fujioka [b] and Rui Sun *[b]

a. *Philipps-Universität Marburg, Fachbereich Chemie, 35032 Marburg, Germany.*

b. *Department of Chemistry, University of Hawai'i at Manoa, Honolulu, Hawaii 96822, United States*

* *Karl-Michael Weitzel, weitzel@chemie.uni-marburg.de*

* *Rui Sun, ruisun@hawaii.edu*

Table of content

1. Single-collision conditions

As mentioned in the main text, single-collision conditions are ensured by setting the HCl/DCl-pressure in the reaction zone (RZ) to $1.15 \cdot 10^{-4}$ mbar. Single-collision conditions are operative, if the mean free path λ_m of the ion is larger than the length l_{RZ} of the RZ:

$$\lambda_m = \frac{k_B \cdot T}{\sigma \cdot p_{RZ}} > l_{RZ} = 25\ cm \qquad \text{(S1)}$$

In the equation S1, p_{RZ} represents the pressure in the RZ. In the current study, cross sections were measured in the E_{cm}-range from 0.12 eV to 5.85 eV. The experimental cross sections lie between approximately 0.003 Å^2 and 35.59 Å^2 in the E_{cm}-range investigated. This leads to a mean free path between 98.9 cm and $1.2 \cdot 10^6$ cm (T = 293.15 K), which is larger than l_{RZ}. Thus, single-collision conditions are ensured.

2. Derivation of the second order rate constants for the HBr^+ + HCl system

The kinetic analysis of data regarding the reaction system HBr^+ + HCl is based on the following rate law of second order, which describes a parallel reaction:

$$\frac{d[\mathrm{HBr}^+]}{dt} = -\left(k_{PT,HCl} + k_{CT}\right) \cdot [\mathrm{HBr}^+] \cdot [HCl] \tag{S2}$$

$k_{PT,HCl}$ and k_{CT} are the rate constants of the proton transfer reaction and charge transfer reaction. Since the particle number density of HCl is much larger than that of HBr^+ ([HCl] >> [HBr^+]), a pseudo-first order rate law can be formulated:

$$\frac{d[\mathrm{HBr}^+]}{dt} = -k'_{\mathrm{tot}} \cdot [\mathrm{HBr}^+] \tag{S3}$$

In the above equation, k'_{tot} represents the total pseudo-first order rate constant:

$$k'_{tot} = \left(k_{PT,HCl} + k_{CT}\right) \cdot [HCl] \tag{S4}$$

By separating the variables and solving the differential equation S3 the integrated rate law S5 is obtained. $[HBr^+]_0$ is the HBr^+ concentration at time $t = 0$.

$$\ln\left(\frac{[HBr^+]_t}{[HBr^+]_0}\right) = -k'_{tot} \cdot t \tag{S5}$$

The HBr^+ concentration at time $t = 0$ is equal to the sum of HBr^+ and the products H_2Cl^+ and HCl^+ at time *t*.

$$[HBr^+]_0 = [HBr^+]_t + [H_2Cl^+]_t + [HCl^+]_t \tag{S6}$$

Inserting S6 into S5 the integrated rate law is independent on the starting concentration of HBr^+.

$$\ln\left(\frac{[HBr^+]_t}{[HBr^+]_t + [H_2Cl^+]_t + [HCl^+]_t}\right) = -k'_{tot} \cdot t \tag{S7}$$

Defining the fractional abundance fa_{HBr^+}, which is the ratio between the concentration of the educt and the sum of the educt and products. In the experiment the concentrations are related to the ion signal intensity I_{HBr^+} of HBr^+ and the sum of the reactant and product ion signal intensities.

$$fa_{HBr^+} = \frac{[HBr^+]_t}{[HBr^+]_t + [H_2Cl^+]_t + [HCl^+]_t} = \frac{I_{HBr^+}}{I_{HBr^+} + I_{H_2Cl^+} + I_{HCl^+}} \tag{S8}$$

Using the expression of equation S8, equation S7 can be simplified to equation S9 and the rate constant can be calculated.

$$k'_{tot} = -\frac{\ln\left(fa_{HBr^+}\right)}{t} \tag{S9}$$

In the next step the rate law of the proton transfer reaction channel is build up.

$$\frac{d[H_2Cl^+]}{dt} = k_{PT,HCl} \cdot [HBr^+] \cdot [HCl] \tag{S10}$$

Assuming [HCl] in excess of $[HBr^+]$ the pseudo-first order rate law in equation S11 is obtained. $k'_{PT,HCl}$ is the pseudo-frist order rate constant of the PT-reaction.

$$\frac{d[H_2Cl^+]}{dt} = k'_{PT,HCl} \cdot [HBr^+] \tag{S11}$$

The integrated rate law in equation S5 is rearranged and then inserted into equation S11.

$$\frac{d[H_2Cl^+]}{dt} = k'_{PT,HCl} \cdot [HBr^+]_0 \cdot \exp\left(-k'_{tot} \cdot t\right) \tag{S12}$$

Subsequently equation S12 is solved by separating the variables and integrating. By integration from t = 0 to *t*, the integrated rate law of the PT-reaction channel is obtained in equation S13.

$$\left[H_2Cl^+\right]_t - \left[H_2Cl^+\right]_0 = \frac{k'_{PT,HCl} \cdot \left[\mathrm{HBr}^+\right]_0}{k'_{tot}} \cdot \left(- \exp\left(- k'_{tot} \cdot t\right) + 1\right) \tag{S13}$$

Since the concentration of H_2Cl^+ at time t = 0 is zero, the second term on the left side of equation S13 vanishes. By dividing equation S13 by $[HBr^+]_0$ and inserting equation S6 leads to the following equation S14.

$$\frac{\left[H_2Cl^+\right]_t}{\left[HBr^+\right]_t + \left[H_2Cl^+\right]_t + \left[HCl^+\right]_t} = \frac{k'_{PT,HCl}}{k'_{tot}} \cdot \left(- \exp\left(- k'_{tot} \cdot t\right) + 1\right) \tag{S14}$$

$$fa_{H_2Cl^+} = \frac{\left[H_2Cl^+\right]_t}{\left[HBr^+\right]_t + \left[H_2Cl^+\right]_t + \left[HCl^+\right]_t} = \frac{I_{H_2Cl^+}}{I_{HBr^+} + I_{H_2Cl^+} + I_{HCl^+}} \tag{S15}$$

The left side of equation S14 is replaced by equation S15, which is the fractional abundance of the H_2Cl^+ product. This is the ratio of the H_2Cl^+ concentration and the concentrations of the educt and products. This is once again related to the corresponding ion signal intensities.

$$k'_{PT,HCl} = \frac{fa_{H_2Cl^+} \cdot k'_{tot}}{\left(- \exp\left(- k'_{tot} \cdot t\right) + 1\right)} \tag{S16}$$

This pseudo-first order rate constant is divided by the concentration of HCl at time *t = 0*, and the rate constant of PT-reaction is obtained.

$$k_{PT,HCl} = \frac{1}{[HCl]_0} \cdot \frac{fa_{H_2Cl^+} \cdot k'_{tot}}{\left(- \exp\left(- k'_{tot} \cdot t\right) + 1\right)} \tag{S17}$$

The calculation of the rate constant of the CT-reaction follows the same approach, only the fractional abundance differs as shown in equation S18.

$$fa_{HCl^+} = \frac{[HCl^+]_t}{[HBr^+]_t + [H_2Cl^+]_t + [HCl^+]_t} = \frac{I_{HBr^+}}{I_{HBr^+} + I_{H_2Cl^+} + I_{HCl^+}} \quad \text{(S18)}$$

The rate constant of the CT-reaction therefor is calculated according to equation S19.

$$k_{CT} = \frac{1}{[HCl]_0} \cdot \frac{fa_{HCl^+} \cdot k'_{tot}}{(-\exp(-k'_{tot} \cdot t) + 1)} \quad \text{(S19)}$$

By dividing the rate constant with the relative velocity the cross section σ can be calculated. Assuming the HCl molecule is at rest the relative velocity is equal to the velocity of the HBr^+ ion.

$$\sigma = \frac{k}{v_{HBr^+}} \quad \text{(S20)}$$

3. Mass spectrum for the reaction $HBr^+ + HCl$

Figure S 1 shows a typical mass spectrum for the reaction system $HBr^+ + HCl$.

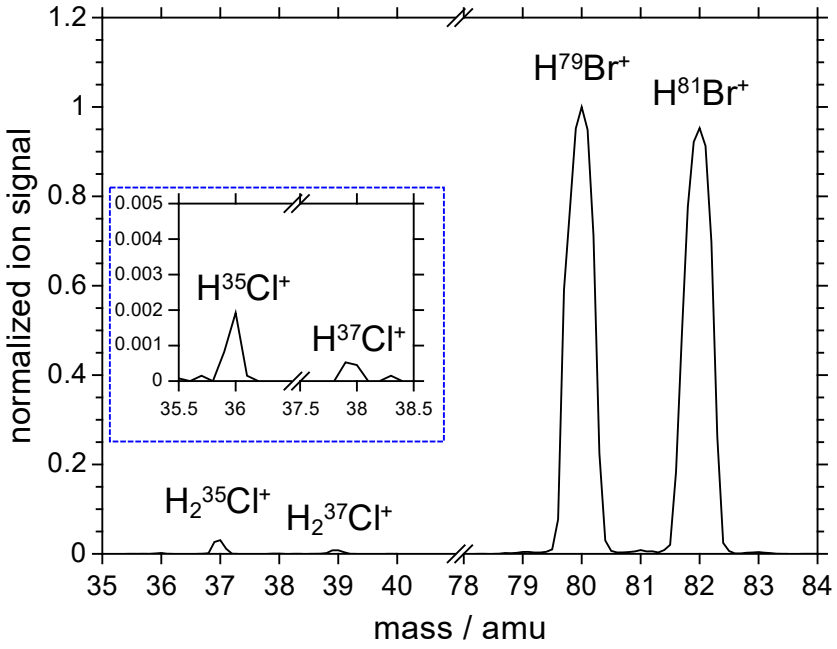

Figure S 1.Mass spectrum for the reaction system $HBr^+ + HCl$, E_{cm} = 4.45 eV, E_{rot} = 3.4 meV.

4. Analysis of signals for $HBr^+ + HCl$

The reactant ions $H^{79}Br^+$ (m = 80 amu) and $H^{81}Br^+$ (m = 82 amu) cause the most intense ion signals in the mass spectrum. The product ions regarding the PT-reaction – $H_2{}^{35}Cl^+$ and $H_2{}^{37}Cl^+$ - appear at m = 37 amu and m = 39 amu respectively. Furthermore, $H^{35}Cl^+$ and $H^{37}Cl^+$ (m = 36 amu and m = 38 amu) represent the product ions of the CT-channel. Hydrogen abstraction (HA) cannot be analyzed, since the corresponding product ions $H_2{}^{79}Br^+$ (m = 81 amu) and $H_2{}^{81}Br^+$ (m = 83 amu) are also formed via the efficient PT/HA-reaction between HBr^+ and HBr.[1] Additionally, the signals of $^{79}Br^+$ and $^{81}Br^+$ (m = 79 amu and m = 81 amu), formed by one-photon dissociation of HBr^+,[2] are part of the mass spectrum.

Based on this spectrum, the ion signals I of HBr^+, HCl^+ and H_2Cl^+ are calculated in the following way (the indices represent the mass):

$$I_{HBr+} = I_{80} + I_{82} \quad \text{(S21)}$$

$$I_{HCl+} = I_{36} + I_{38} \quad \text{(S22)}$$

$$I_{H_2Cl+} = I_{37} + I_{39} \quad \text{(S23)}$$

These ion signals are used to calculate the fractional abundance according to equations S8, S15 and S18. Subsequently the rate constants are calculated as presented in the section 2.

5. Derivation of the second order rate constants for the HBr^+ + DCl system

The kinetic analysis of data regarding the reaction system HBr^+ + DCl is based on the following rate law of second order, which describes a parallel reaction:

$$\frac{d[\mathrm{HBr}^+]}{dt} = -\left(k_{PT,DCl} + k_{DA}\right) \cdot [\mathrm{HBr}^+] \cdot [DCl] \tag{S24}$$

$k_{PT,DCl}$ and k_{DA} are the rate constants of the proton transfer reaction and deuterium abstraction reaction. Since the particle number density of DCl is much larger than that of HBr^+ ([DCl] >> [HBr^+]), a pseudo-first order rate law can be formulated:

$$\frac{d[\mathrm{HBr}^+]}{dt} = -k'_{\mathrm{tot}} \cdot [\mathrm{HBr}^+] \tag{S25}$$

In the above equation, k'_{tot} represents the total pseudo-first order rate constant:

$$k'_{tot} = \left(k_{PT,DCl} + k_{DA}\right) \cdot [DCl] \tag{S26}$$

By separating the variables and solving the differential equation S25 the integrated rate law S27 is obtained. $[HBr^+]_0$ is the HBr^+ concentration at time $t = 0$.

$$\ln\left(\frac{[HBr^+]_t}{[HBr^+]_0}\right) = -k'_{tot} \cdot t \tag{S27}$$

The HBr^+ concentration at time $t = 0$ is equal to the sum of HBr^+ and the products $HDCl^+$ and $HDBr^+$ at time t.

$$[HBr^+]_0 = [HBr^+]_t + [HDCl^+]_t + [HDBr^+]_t \tag{S28}$$

Inserting S28 into S27 the integrated rate law is independent on the starting concentration of HBr^+.

$$\ln\left(\frac{[HBr^+]_t}{[HBr^+]_t + [HDCl^+]_t + [HDBr^+]_t}\right) = -k'_{tot} \cdot t \tag{S29}$$

Defining the fractional abundance fa_{HBr^+}, which is the ratio between the concentration of the educt and the sum of the educt and products. In the experiment the concentrations are related to the ion signal intensity I_{HBr^+} of HBr^+ and the sum of the reactant and product ion signal intensities.

$$fa_{HBr^+} = \frac{[HBr^+]_t}{[HBr^+]_t + [HDCl^+]_t + [HDBr^+]_t} = \frac{I_{HBr^+}}{I_{HBr^+} + I_{HDCl^+} + I_{HDBr^+}} \tag{S30}$$

Using the expression of equation S30, equation S29 can be simplified to equation S31 and the rate constant can be calculated.

$$k'_{tot} = -\frac{\ln\left(fa_{HBr^+}\right)}{t} \tag{S31}$$

In the next step the rate law of the proton transfer reaction channel is build up.

$$\frac{d[HDCl^+]}{dt} = k_{PT,DCl} \cdot [HBr^+] \cdot [DCl] \tag{S32}$$

Assuming [DCl] in excess of $[HBr^+]$ the pseudo-first order rate law in equation S33 is obtained. $k'_{PT,DCl}$ is the pseudo-first order rate constant of the PT-reaction.

$$\frac{d[HDCl^+]}{dt} = k'_{PT,DCl} \cdot [HBr^+] \tag{S33}$$

The integrated rate law in equation S27 is rearranged and then inserted into equation S33.

$$\frac{d[HDCl^+]}{dt} = k'_{PT,DCl} \cdot [\mathrm{HBr}^+]_0 \cdot \exp\left(-k'_{tot} \cdot t\right) \tag{S34}$$

Subsequently equation S34 is solved by separating the variables and integrating. By integration from $t = 0$ to t, the integrated rate law of the PT-reaction channel is obtained in equation S35.

$$[HDCl^+]_t - [HDCl^+]_0 = \frac{k'_{PT,DCl} \cdot [\mathrm{HBr}^+]_0}{k'_{tot}} \cdot (-\exp\left(-k'_{tot} \cdot t\right) + 1) \tag{S35}$$

Since the concentration of H_2Cl^+ at time $t = 0$ is zero, the second term on the left side of equation S35 vanishes. By dividing equation S35 by $[HBr^+]_0$ and inserting equation S28 leads to the following equation S36.

$$\frac{[HDCl^+]_t}{[HBr^+]_t + [HDCl^+]_t + [HDBr^+]_t} = \frac{k'_{PT,DCl}}{k'_{tot}} \cdot (-\exp\left(-k'_{tot} \cdot t\right) + 1) \tag{S36}$$

$$fa_{HDCl^+} = \frac{[HDCl^+]_t}{[HBr^+]_t + [HDCl^+]_t + [HDBr^+]_t} = \frac{I_{HDCl^+}}{I_{HBr^+} + I_{HDCl^+} + I_{HD}} \tag{S37}$$

The left side of equation S36 is replaced by equation S37, which is the fractional abundance of the H_2Cl^+ product. This is the ratio of the H_2Cl^+ concentration and the concentrations of the educt and products. This is once again related to the corresponding ion signal intensities.

$$k'_{PT,DCl} = \frac{fa_{HDCl^+} \cdot k'_{tot}}{(-\exp\left(-k'_{tot} \cdot t\right) + 1)} \tag{S38}$$

This pseudo-first order rate constant is divided by the concentration of HCl at time $t = 0$, and the rate constant of PT-reaction is obtained.

$$k_{PT,DCl} = \frac{1}{[DCl]_0} \cdot \frac{fa_{HDCl^+} \cdot k'_{tot}}{(-\exp(-k'_{tot} \cdot t) + 1)} \quad \text{(S39)}$$

The calculation of the rate constant of the DA-reaction follows the same approach, only the fractional abundance differs as shown in equation S40.

$$fa_{HDBr^+} = \frac{[HDBr^+]_t}{[HBr^+]_t + [HDCl^+]_t + [HDBr^+]_t} = \frac{I_{HDBr^+}}{I_{HBr^+} + I_{HDCl^+} + I_{HD}} \quad \text{(S40)}$$

The rate constant of the DA-reaction therefor is calculated according to equation S41.

$$k_{DA} = \frac{1}{[DCl]_0} \cdot \frac{fa_{HDBr^+} \cdot k'_{tot}}{(-\exp(-k'_{tot} \cdot t) + 1)} \quad \text{(S41)}$$

By dividing the rate constant with the relative velocity the cross section σ can be calculated. Assuming the DCl molecule is at rest the relative velocity is equal to the velocity of the HBr^+ ion.

$$\sigma = \frac{k}{v_{HBr^+}} \quad \text{(S20)}$$

6. Mass spectrum for the reaction $HBr^+ + DCl$

Figure S 2 shows a typical mass spectrum for the reaction system $HBr^+ + DCl$.

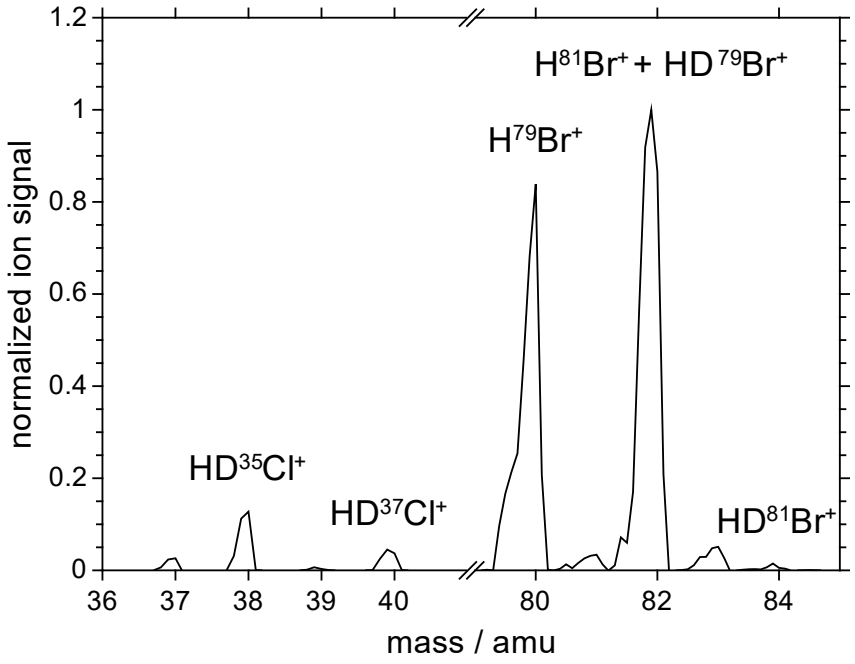

Figure S 2.Mass spectrum for the reaction system $HBr^+ + DCl$, Ecm = 0.26 eV, Erot = 3.4 meV.

7. Analysis of signals for $HBr^+ + DCl$

Just as in case of $HBr^+ + HCl$, the reactant ions $H^{79}Br^+$ (m = 80 amu) and $H^{81}Br^+$ (m = 82 amu) cause the most intense ion signals in the mass spectrum. The $H^{81}Br^+$-signal overlaps with the $HD^{79}Br^+$-signal, which represents a product ion resulting from deuterium abstraction (DA). At m = 38 amu and m = 40 amu, the product ion signals of proton transfer (PT) – $HD^{35}Cl^+$ and $HD^{37}Cl^+$ – appear. The CT-products $D^{35}Cl^+$ and $D^{37}Cl^+$ (m = 37 amu and m = 39 amu) overlap with $H_2{}^{35}Cl^+$ and $H_2{}^{37}Cl^+$. Hence, the charge transfer cannot be analyzed. The ions $H_2{}^{35}Cl^+$ and $H_2{}^{37}Cl^+$ originate from the efficient proton transfer between HBr^+ and HCl. Hydrogen chloride is present in the apparatus because of the specification of the used DCl-lecture bottle (Sigma-Aldrich, 99 atom % D) as well as due to the isotope exchange HBr + DCl ↔ DBr + HCl. In contrast to the $HBr^+ + HCl$-system, $H_2{}^{79}Br^+$ and $H_2{}^{81}Br^+$ (m = 81 amu and m = 83 amu) are no disruptive factor. The H_2Br^+-signals in Figure S 2 are more intense compared to Figure S 1. This results from the fact that the mass spectrum depicted in Figure S 2 is based on a lower collision energy (exothermic PT/HA-reaction between HBr^+ and HBr[3]).

Concerning the $HBr^+ + DCl$-system, the ion signal of $HDCl^+$ is calculated as follows:

$$I_{HDCl^+} = I_{38} + I_{40} \tag{S42}$$

The ratio of the $H^{81}Br^+$ signal and the $HD^{79}Br^+$ signal can be calculated with equation S6, where Q_{Br} represents the natural isotope ratio $^{81}Br/^{79}Br = 0.973$.

$$I_{HD^{79}Br^+} = \frac{I_{H^{81}Br^+}}{\frac{I_{H^{79}Br^+}}{I_{HD^{81}Br^+} \cdot Q_{Br}^2}} \tag{S43}$$

Based on this relation, the ion signals of HBr^+ and $HDBr^+$ are calculated with the equations S21 and S22:

$$I_{HBr^+} = I_{80} + \frac{I_{82}}{\frac{I_{84}}{I_{80}} \cdot Q_{Br}^{-2} + 1} \tag{S44}$$

$$I_{HDBr^+} = \frac{I_{82}}{\frac{I_{80}}{I_{84}} \cdot Q_{Br}^{2} + 1} + I_{84} \tag{S45}$$

These ion signals are used to calculate the fractional abundance according to equations S30, S37 and S40. Subsequently the rate constants are calculated as presented in the section 5.

8. $HBr^+ + HCl$ normalized cross sections

In order to compare the steepness of the collision energy dependence of experimental and theoretical cross sections a look at normalized representations is instructive. In Figure S 3 the cross sections normalized to $\sigma(E_{cm} = 0.25\ eV)$, i.e. the lowest experimental collision energy, are plotted as a function of the collision energy for the PT_{HCl}-reaction. In Figure S 4 the cross sections normalized to $\sigma(E_{cm} = 5.85\ eV)$, i.e. the largest experimental collision energy, are plotted. Both graphs show the experimental data at various rotational energies and the Langevin result. Since the Langevin, the ADO and the SC calculations all have the same energy dependence and only differ by a numerical factor, their normalized representations fall on top of each other.

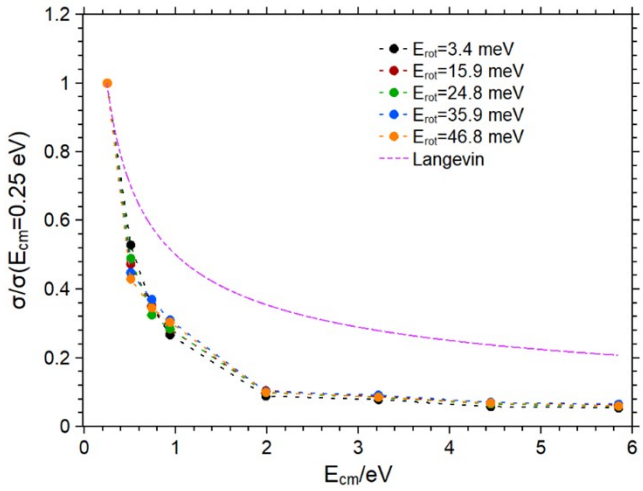

Figure S 3. Normalized cross sections for the PT_{HCl}-reaction as a function of the collision energy. The different traces correspond to different rotational energies.

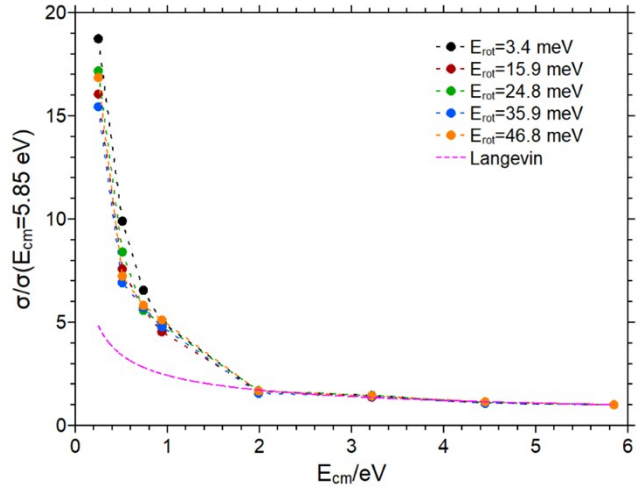

Figure S 4. Normalized cross sections for the PT_{HCl}-reaction as a function of the collision energy. The different traces correspond to different rotational energies.

Figure S 3 illustrates that the energy dependence of the experimental cross sections is overall much steeper than predicted by the classical theoretical models. Figure S 4 illustrates that the variation of experimental cross sections with collision energy matches the one predicted by the Langevin – model for collision energies above 2 eV, if normalized at large energies. The difference in the steepness between experimental data and Langevin model is also quantified by the n – parameter of the fit function according to eq. 5 given in the main text. This difference is most obvious at small collision energies.

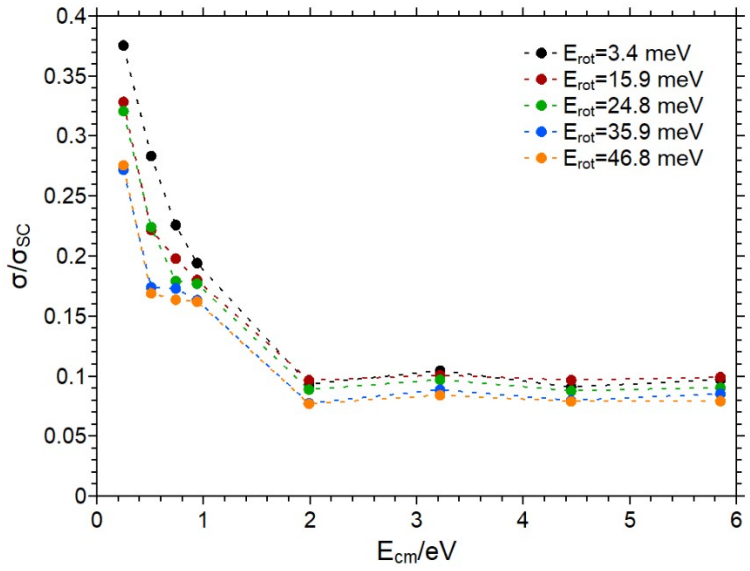

Figure S 5. Experimental cross sections divided by the cross section according to the SC – model. The different traces correspond to the different rotational energies of the cation.

As yet another illustration, Figure S 5 presents the experimental cross section of the PTHCl reaction divided by the SC – model cross section as function of the collision energy. The SC – model predicts a constant factor for the ratio of the capture cross section and the Langevin – model cross section. In case of the PTHCl reaction this factor is bigger than predicted by the SC – model. Below the collision energy of 2 eV the ratio increases. On the other hand, for collsion energies above 2 eV (there the normalized experimental cross sections approach to the normalized Langevin – model) the ratio is constant. But it is larger than predicted by the SC – model.

9. HBr^+ + DCl normalized cross sections

As a complementation, In Figure S 6 and Figure S 7, the cross section, normalized to $\sigma(E_{cm}$ = 0.12 eV) and $\sigma(E_{cm}$ = 2.03 eV) respectively is plotted as a function of the collision energy for the PT_{DCl}-reaction. The normalized cross sections are compared to the normalized Langevin – model to illustrate the relative evolution of the experimental and theoretical cross sections. For all rotational energies investigated, the PT_{DCl} – reaction cross section decreases steeper with decreasing collision energy than predicted by the Langevin – model. This basically applies in the entire range of collision energies investigated. In other words, at the largest collision energy considered the cross section has not yet reached the effective high energy limit.

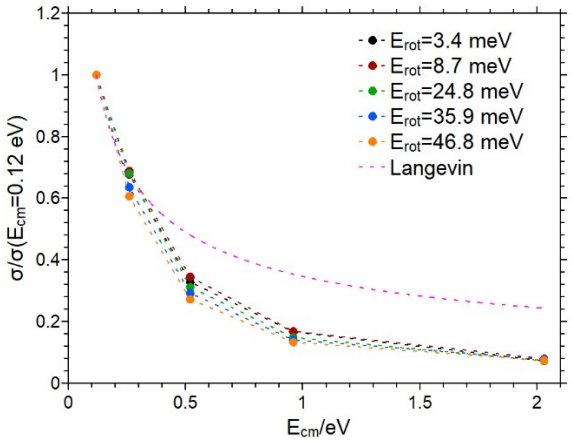

Figure S 6. Normalized cross sections for the PT_{DCl}-reaction as a function of the collision energy. The different traces correspond to different rotational energies. The cross sections are normalized to the lowest experimental collision energy.

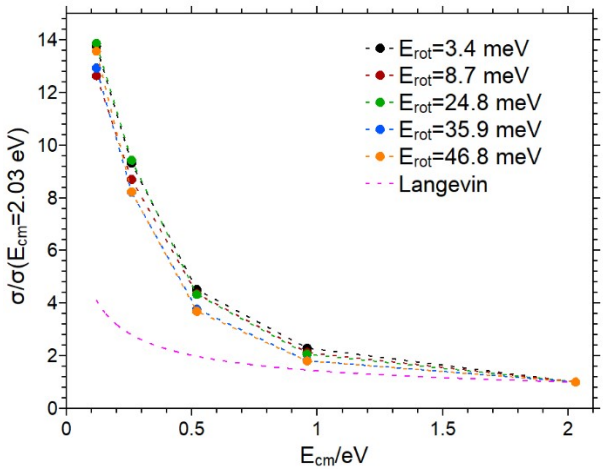

Figure S 7. Normalized cross sections for the PT_{DCl}-reaction as a function of the collision energy. The different traces correspond to different rotational energies. The cross sections are normalized to the highest experimental collision energy.

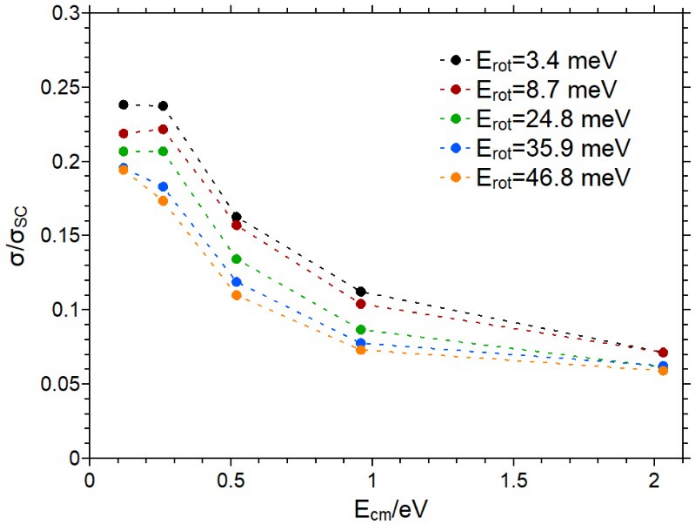

Figure S 8. PT_{DCl} cross section divided by the SC – model cross section as a function of the collision energy.

In Figure S 8 the experimental cross section normalized to the SC – model is shown as a function of the collision energy. As in section 8 discussed the ratio of the capture cross section and the Langevin cross section is expected to be constant according to the SC – model. This is only observed in the range from 0.12 eV to 0.26 eV for the three lowest rotational energies. In the other investigated energy ranges this quotient decreases monotonically.

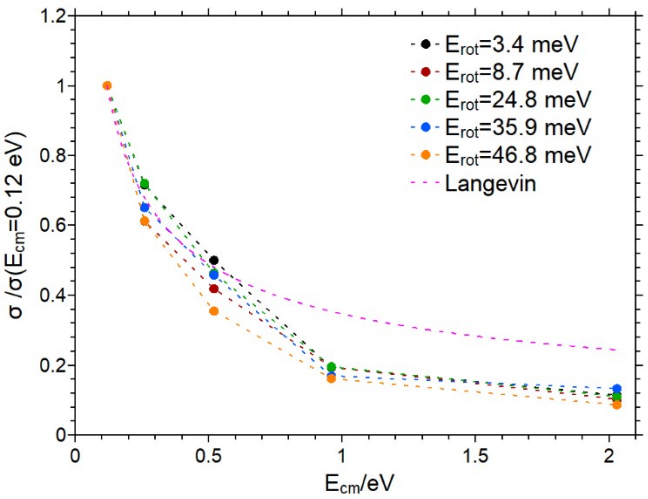

Figure S 9. Normalized cross sections for the DA-reaction as a function of the collision energy. The different traces correspond to different rotational energies. The cross sections are normalized to the lowest experimental collision energy.

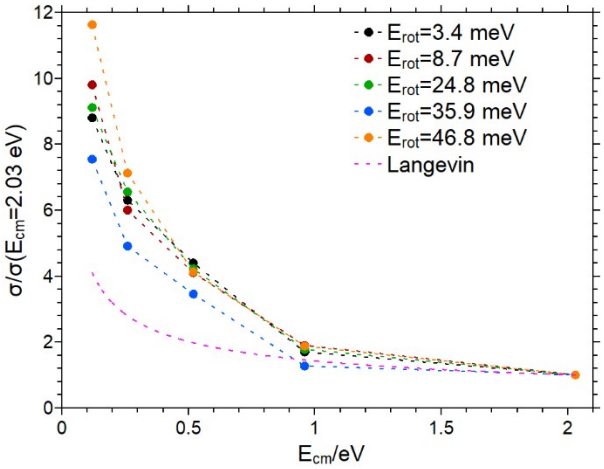

Figure S 10. Normalized cross sections for the DA-reaction as a function of the collision energy. The different traces correspond to different rotational energies. The cross sections are normalized to the highest experimental collision energy.

Figure S 9 and Figure S 10 show the experimental cross sections for the DA – reaction normalized to the lowest and highest collision energy respectively. Depending on the normalization the experimental traces runs closer to the Langevin – model in the range of lower or higher collision energies. Both figures illustrate therefor the steeper decrease of the experimental cross section compared to the one predicted by the Langevin – model.

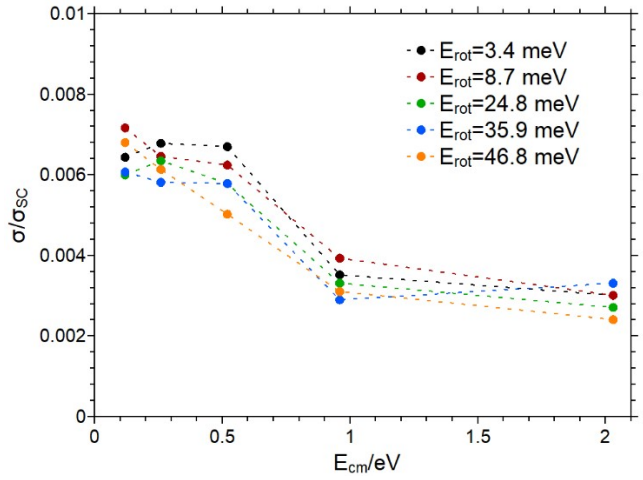

Figure S 11. PTDCl cross section divided by the SC – model cross section as a function of the collision energy.

Figure S 11 shows the experimental cross section normalized to the SC – model. As the SC – model predicts the ratio of the capture cross section and the Langevin cross section should be constant. This is observed for the DA – reaction for the lower collision energies (0.12 eV to 0.5 eV) expect for the highest rotational energy and in the collision energy range from 0.96 eV up to 2.03 eV for all rotational energies. Between 0.5 eV and 0.96 eV the proportionality factor changes.

10. Comparison of AIMD cross sections of $HBr^+ + HCl$ and $HCl^+ + HCl$

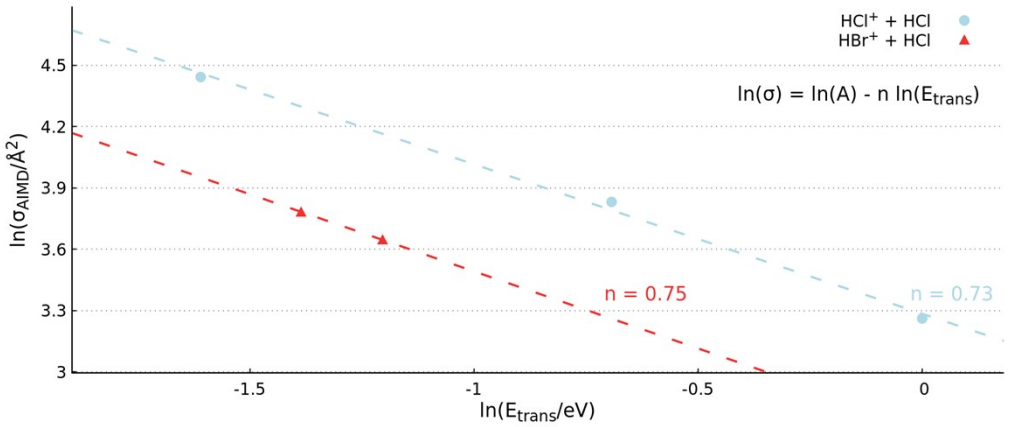

Figure S 12.. Comparison of AIMD cross sections for the titled reaction, $HBr^+ + HCl$ (light red), to a previous similar reaction, $HCl^+ + HCl$ (light blue) at various collision energy. Initial rotational excitations of the cation are zero for both. Fits are based on the theoretical $\sigma = A\ (E_{trans})^{-n}$ power relation.

Figure S12 shows how the collision energy (E_{trans}, x-axis) and reactive PT cross section (σ, y-axis) are related for the J=0 (zero rotational energy) collision. In a log-log graph, the power relation $\sigma = A/(E_{trans})^{-n}$ transforms to $\ln(\sigma) = \ln(A) - n\ \ln(E_{trans})$. Here, the previous reaction HCl^+ and HCl produced an n = 0.73 fit which is nearly replicated with an n = 0.75 fit for the title reaction of the current work.

11. References

(1) Schmidt, S.; Plamper, D.; Jekkel, J.; Weitzel, K.-M. Self-Reactions in the HBr^+ (DBr^+) + HBr System: A State-Selective Investigation of the Role of Rotation. *J. Phys. Chem. A* **2020**, *124*, 8461–8468.

(2) Penno, M.; Holzwarth, A.; Weitzel, K.-M. State selective predissociation spectroscopy of hydrogen bromide ions (HBr^+) via the $^2\Sigma^+ \leftarrow {}^2\Pi_i$(i=1/2, 3/2) transition. *J. Phys. Chem. A* **1998**, *102*, 1927–1934.